EVALUATION OF IMPULSIVE RESPONSE OF RECTANGULAR LIQUID CONTAINERS AGAINST EARTHQAKE EXCITATIONS

A Thesis
Submitted by

SUBHAJOY DATTA
(Roll no.-002010402020)
Reg. No.: 153976 of 20-21
Exam Roll No. - M4CIV22020

In partial fulfilment of the requirements
for the award of the degree of

Master of Engineering
In
Civil Engineering
(Structural Engineering)

Under the Guidance of
Dr. Kalyan Kumar Mandal

Department Of Civil Engineering
Jadavpur University
Kolkata-700032
August-2022

DEPARTMENT OF CIVIL ENGINEERING

FACULTY OF ENGINEERING AND TECHNOLOGY
JADAVPUR UNIVERSITY
KOLKATA – 700 032

CERTIFICATE OF RECOMMENDATION

This is to certify that the thesis entitled, "**EVALUATION OF IMPULSIVE RESPONSE OF RECTANGULAR LIQUID CONTAINERS AGAINST EARTHQUAKE EXCITATIONS**" submitted by **SUBHAJOY DATTA**, Class Roll No. 002010402020, Registration No. 153976 of 20-21 in partial fulfilment of the requirements for the award of Master of Engineering degree in Civil Engineering with specialization in "Structural Engineering" at Jadavpur University, Kolkata is an authentic work carried out by him under my supervision and guidance.
I hereby recommend that the thesis be accepted in partial fulfilment of the requirements for awarding the degree of **"Master of Engineering in Civil Engineering (Structural Engineering)"**.

KKMandal 22/08/2022

Prof. Dr. Kalyan Kumar Mandal
Associate Professor
Department of Civil Engineering
Jadavpur University
Kolkata- 700032

Associate Professor
Department of Civil Engineering
Jadavpur University
Kolkata-700 032

Chakraborty 22/08/22

Prof. Dr. Shibnath Chakraborty
Head of the Department
Department of Civil Engineering
Jadavpur University
Kolkata- 700032

Head
Department of Civil Engineering
Jadavpur University
Kolkata-700 032

22/8/22

Prof. Dr. Chandan Mazumdar
DEAN, FET
Jadavpur University
Kolkata- 700032

DEAN
Faculty of Engineering & Technology
JADAVPUR UNIVERSITY
KOLKATA-700 032

DEPARTMENT OF CIVIL ENGINEERING
FACULTY OF ENGINEERING AND TECHNOLOGY
JADAVPUR UNIVERSITY
KOLKATA – 700 032

CERTIFICATE OF APPROVAL

This thesis paper is hereby approved as a credible study of an engineering subject carried out and presented in a manner satisfactorily to warrant its acceptance as a pre-requisite for the degree for which it has been submitted. It is understood that, by this approval the undersigned do not necessarily endorse or approve any statement made, opinion expressed or conclusion drawn therein but approved the thesis paper only for the purpose for which it is submitted.

Committee of Thesis Paper Examiners

_____

Signature of Examiner

_____

Signature of Examiner

DECLARATION

I, Subhajoy Datta, Master of Engineering in Civil Engineering (Structural Engineering), Jadavpur University, Faculty of Engineering & Technology, hereby declare that the work being presented in the thesis work entitled, "**Evaluation of Impulsive Response of Rectangular Liquid Containers Against Earthquake Excitations**" is authentic record of work that has been carried out at the Department of Civil Engineering, Jadavpur University, Kolkata under the guidance of Dr. Kalyan Kumar Mandal, Associate Professor, Department of Civil Engineering, Jadavpur University. The work contained in the thesis has not yet been submitted in part or full to any other university or institution or professional body for award of any degree or diploma or any fellowship.

Subhajoy Datta

Place: Kolkata
Date: 22.08.2022

Subhajoy Datta
Class Roll: 002010402020
Reg. No.: 153976 of 20-21

ACKNOWLEDGEMENT

I gratefully acknowledge the resourceful guidance, active supervision and constant encouragement of our reverent Associate Professor **Dr. Kalyan Kumar Mandal** of the Department of Civil Engineering, Jadavpur University, Kolkata, who despite his other commitments could find time to help me in bringing this thesis to its present shape. I do convey my sincere thanks and gratitude to him.

I also thankfully acknowledge my gratefulness to all Professors and staffs of Civil Engineering Department, Jadavpur University, Kolkata, for extending all facilities to carry out the present study.

I also thankfully acknowledge the assistance and encouragement received from my family members, friends and others during the preparation of this Thesis.

Subhajoy Datta

Place: Kolkata
Date: 22.08.2022

Subhajoy Datta
Roll No.: 002010402020
Regist. No.: 153976 of 20-21

ABSTRACT

The impulsive hydrodynamic pressure exerted by the fluid on walls of rectangular tanks due to excitations of different frequencies during two different earthquakes, is investigated by pressure based finite element method. The tank walls are assumed to be rigid. The fluid inside is considered as water. The fluid within the tank is considered as inviscid and fluid motion is irrotational. The finite element formulation of wave equation is done by Galerkin approach. Newmark's average integration method, which is considered as unconditionally stable, has been used to obtain the response in time domain. The present algorithm does not include the compressibility of water in the reservoir.

The efficacy of the present algorithm has been demonstrated through numerous examples. The impulsive hydrodynamic pressure increases with the increase of exciting frequency and has maximum value at the bottom of the tank. Hydrodynamic pressure at the free surface is independent to the height of fluid. However, the pressure at base and mid height of vertical wall depends on height of fluid. At these two locations, the impulsive hydrodynamic pressure increases with the increase of fluid depth. The depth of undisturbed fluid near the base increases with the increase of depth of fluid when it is excited with fundamental frequency of fluid. The impulsive hydrodynamic pressure at a constant depth increases with the increase of height of the tank. Due to the earthquake excitations, the fluid gets disturbed but the disturbance is maximum at the free surface of the fluid and minimum at the base of the tank.

KEYWORDS: *Compressibility of water, Finite element method, Impulsive Hydrodynamic Pressure, Fundamental frequency, Sloshed Displacement*

LIST OF SYMBOLS

Symbols	Description
a	Acceleration of excitation
Amp	Amplitude of excitation
C	Acoustic wave speed
C_P	Hydrodynamic pressure coefficient
g	Gravitational acceleration
H	Height of fluid, Height of tank
L	Length of the tank
ρ	Mass density of fluid
N_t	No of time steps
N_h	Nos. of horizontal division of mesh
N_v	Nos. of vertical division of mesh
P	Hydrodynamic Pressure
T	Time period of excitation
V_t	Velocity of fluid at time t
U_t	Displacement of fluid at time t
W	Exciting frequency
w	Fundamental frequency of water within tank

CONTENTS

List of Figures

List of Tables

CHAPTER 1
INTRODUCTION

1.1 GENERAL

Tanks are commonly used to store water and various fluids in the oil industry. Damage in tanks may cause a loss of liquid content, which could result in economic damage, as well as in long-term contamination of soil for tanks resting on soil. The sloshing effect and the hydrodynamic pressure act on walls are the major guiding parameters in the design of such tanks. The clear understanding of sloshing characteristics is essential for the determination of required freeboard to prevent overflow the fluid and also for the estimation of hydrodynamic pressure on the fluid retaining container such as tank. It is also very important for water storage tank using for cooling in nuclear plant and fire demand supply, which has to withstand during earthquake. Different types of numerical schemes, such as the finite difference method, the finite volume method, the boundary element method and finite element method may be used to obtain the responses of the fluid within the tank.

The analysis of water tank is an example of fluid-structure interaction problem or in other word, the proper and precise responses of the tank is obtained if the fluid-structure interaction effect is considered in the analysis. Further, the responses will be so realistic if this problem is dealt in 3D. However, in existing literatures it is reported that the effect of the flexibility of the tank does not change the pressure distribution if the tank wall is sufficiently thick. Therefore, the assumption of rigid tank is a good approximation to evaluate the hydrodynamic pressures due to the sloshing component of the liquid in tanks. Similarly, 2D approximation of rectangular water tank may be considered for a certain value of width to length ratio of rectangular tanks.

The Hydrodynamic pressure exerted by the fluid on the tank wall and amplitude of slosh depends on the amplitude and frequency of the tank motion, liquid depth, liquid properties, tank geometry, and also the size, shape and location of the internal baffle. Abundant research has been carried out on the seismic response of cylindrical liquid storage tanks mainly to know the sloshing behavior and mode shape but very few contributions have been published for determining total hydrodynamic pressure of rectangular tank and analysis is carried out considering fluid as

incompressible, irrotational and inviscid. However, the compressibility effect of fluid may plays an important role for precise estimation of total hydrodynamic pressure and the sloshed deformation for calculation of free board in tanks.

1.2 Objective

The objectives of this study are firstly, to develop a 2D finite element algorithm for obtaining responses of rectangular tank considering water to be compressible and secondly, to develop a finite element algorithm for obtaining the impulsive responses against different earthquake excitations.

CHAPTER 2

LITERATURE REVIEW

2.1 GENERAL

To provide a detailed review of the literature related to the dynamic analysis of liquid storage tank in its entire would be difficult to address in this chapter. A brief review of previous studies about dynamic analysis of liquid storage tank is presented in this section which are related to the present study. This literature review focuses on recent contributions related to this work and past efforts most closely related to the needs of the present work.

2.2 LITERATURE REVIEW

A comparative study of Draft IS 1893 Part 2, ACI 350.3 and Eurocode 8 for rectangular tanks was carried out by **Kumar et al. (2015).** Both impulsive and convective components were considered to determine the hydrodynamic pressure and proposed different charts for design seismic forces and sloshing.

Jung et al. (2012) suggested the effect of height of vertical baffle on the liquid sloshing in a laterally moving three-dimensional rectangular tank. The study highlighted the time variation of pressure, the mean maximum pressure and the free surface elevation in relation to the baffle height. The liquid sloshing is getting more suppressed with the increase of baffle height.

The dynamic analysis of rectangular tank using response spectra to find out deformation and bending moment of walls was carried out by **Uhlirova and Jendzelovsky (2019)**. The paper emphasized the need of considering liquid filling as a part of structure rather than a static load. The study also showed the different natures of deformation and bending moments in walls depended on the direction of external load.

Mi-an et al. (2013) designed and built an experiment to study the effects of Perforated Baffle on reducing sloshing in rectangular tank and established the relationship between free surface elevation and pressure distribution with changing external frequency. The study showed that the damping effect of vertical baffle wall was more effective in lower external frequency. However, the perforated baffle was effective in reducing sloshing at higher external frequency.

Sloshing with a vertical baffle in a moving partially filled rectangular tank was evaluated by **Akyildiz (2012)**. A numerical algorithm was proposed to study the non-linear behavior of liquid sloshing. The study found the critical baffle height for liquid to reach the roof of the tank and also the flow separation with changing baffle height and concluded that with the increase of baffle height, the liquid sloshing was suppressed and the vortex size and strength became smaller and weaker.

Chen et al. (2009) performed a numerical simulation of liquid sloshing in partially filled containers using proper boundary conditions to calculate the impact pressure. Boundary conditions are adopted as usually taken to solve Navier-Strokes or Euler's equation. Sloshing effect is assessed numerically at different filling levels and excitation frequencies. The study adopted two fluid approach that eliminated the requirement of describing free surface.

The experimental study on pressure distribution and 3D effects of liquid sloshing loads on tanks was carried out by **Akyildiz and Unal (2005)**. The experimental set up is designed to validate the results obtained from analytical and numerical solutions. Several conditions of baffled and unbaffled tanks had been studied in this experiment. The paper concluded that baffles significantly reduce fluid motion.

Pal and Bhattacharyya (2010) have studied numerically and experimentally the sloshing effect on partially filled container due to external excitation. This paper has used Meshless local Petrov–Galerkin method to compute the nonlinear sloshing response of liquid in a 2D rigid prismatic tank. By analysing numerical and experimental data, they have concluded that the slosh characteristics are strongly influenced by the tank geometry, depth of liquid, and the amplitude and frequency of external excitation.

A study on non-linear sloshing response by finite element method in a 2D rigid tank with rigid baffles has been done by **Biswal et al. (2006)**. The formulation was being done by a mixed Eulerian–Langrangian scheme and it was solved using the Galerkin method. This paper has adopted a regridding technique to avoid artificial smoothing of free surface. It has examined the effect of baffle dimension, position and number on non-linear sloshing response.

Singh and Singh (2014) have focused on fluid structure interaction in an elliptical tank. The paper has studied the effect of horizontal and vertical baffles individually and concluded that a combination of both is more effective in controlling sloshing than an individual vertical baffle.

The numerical and experimental study on pressure variation and 3D effects on liquid sloshing loads in a partially filled tank was carried out by **Akyildiz and Unal (2006)**. Both the conditions of baffled and unbaffled have been computed numerically and then compared with experimental results. The paper has suggested several conclusions related to sloshing, tank geometry and excitation frequency and suggested more extensive experiments to validate numerical results.

Kim (2001) simulated the effect of sloshing flows in two and three-dimensional containers based on finite difference method. He developed Navier-Stokes equation with free boundary and assumed the free surface to be a single-valued function. The paper has introduced a concept of buffer zone near roof ceiling for a mixed boundary condition before the impact of free surface and rigid roof. The numerical and experimental data are considerably similar.

The Fluid Structure Interaction in partially filled liquid containers was modelled by **Nicolici and Bilegan (2013)**. They have modelled fluid and tank-wall interaction considering full and one-way coupling. The results were compared with simplified mechanical models given in the codes. The paper has concluded that considering one-way coupling may have underpredict the sloshing effect in a partially filled container.

Liu and Lin (2009) have developed a numerical model to study 3D sloshing in a tank with baffles. They have developed the baffles using the concept of Virtual Boundary Force. They validated the results with 2D unbaffled water tank. The paper concluded that vertical baffles are very effective in reducing the sloshing.

The liquid sloshing behaviour of 2D rectangular tank under external excitation was simulated using a standard software by **Hou et al. (2012)**. Their study showed that the coupled excitation can significantly increase the sloshing load and can have violent impact on top wall of the tank.

Kotrasova et al. (2020) studied the time dependent response of the fluid pressure in fluid domain. The peak value of hydrodynamic pressure is calculated by numerical simulation by using FEM. The paper found out that the highest response occurs at the bottom of fluid domain.

The effects of compressibility and surface sloshing motion using the three-dimensional Lagrangian fluid finite element in liquid storage tanks was calculated by

Dogangun et al. (1996). The paper focused on the difference of hydrodynamic pressure on rigid and flexible walls and found out that pressure on flexible walls is larger than rigid walls. The paper concluded that to generalise the results, experiments should be done on more models.

Chen et al. (2009) simulated the liquid sloshing effect in partially filled containers. They have taken the free surface as two different mediums i.e water and air. The paper has found that the interface thickness for smooth transition from one medium to another affects the impact pressure on the roof. The mesh size should be fine enough to accurately predict wave motion and impact on roof at low filling levels.

The two-phase interface was being treated as a physical discontinuity by **Ming and Duan (2010)** for simulation of sloshing in a sway tank. This paper has suggested a finite volume high order numerical algorithm to simulate sloshing on hybrid unstructured grid based on Normalized Variable Diagram. This method can simulate free surface and wave height change reasonably when compared to experimental data.

Mitra and Sinhamahapatra (2008) had dealt with pressure-based finite element analysis of fluid–structure systems considering the coupled fluid and structural dynamics. The fluid-structure interaction analysis is significantly improved by considering coupling phenomena. The bending moment due to pressure distribution and the sloshing motion increases with the increase in wall flexibility.

2.3 CRITICAL OBSERVATION BASED ON LITERATURE REVIEW

Based on the review of literatures, some critical observations are acknowledged. These observations are described below.

- Finite element analysis is recognized to be one of the numerical tool for dynamic analysis of water tanks.
- The water within the tank is expressed by several variables such as displacement, velocity potential and pressure. Out of these variables, it is advantageous to model the fluid within the tank by pressure, as the number of degrees of freedom per mode in this case reduced to one.
- In pressure based formulation, the number of unknown per node is only one. Thus it requires less storage place and computational time.

- In pressure based formulation, fluid satisfies the irrotational condition automatically. Otherwise, a complicated condition has to be incorporated to satisfy the irrotationality condition.
- For dynamic analysis of water tank, the water within the tank may be modeled either as compressible or incompressible fluid.
- Linear and nonlinear wave theory may be used to model the reservoir. However, for water with comparatively smaller depth, linear wave theory is sufficient.
- At a certain limit of width to length ratio (B/L) the performance of tank in 2-D and 3-D are almost similar.
- The sloshed displacement of liquid depends on the tank size and the baffle within the tank.

2.4 Scope of present work

In order to realize the objective of the present work, the scope of the present research has been defined as follows:

- Development of pressure based 2-D finite element formulation of water within the rectangular tank.
- Evaluation of impulsive hydrodynamic pressure on the tank walls for different sizes of containers against earthquake excitations.

CHAPTER 3
THEORETICAL FORMULATIONS

3.1 Theoretical Formulation

The state of stress for a fluid which follows the Newton's law is defined by an isotropic tensor as

$$T_{ij} = -p\delta_{ij} + V_{ij} \quad (3.1)$$

Where, total stress is denoted as T_{ij}, viscous stress tensor is denoted as V_{ij} which is depended only on the rate of change of deformation in such a manner that the value is zero when the fluid is under rigid body motion or rest. The variable p is defined as hydrodynamic pressure which is independent explicitly on the rate of the deformation and δ_{ij} is known as Kronecker Delta. For isotropic linear elastic material viscous stress tensor, V_{ij} can be written as

$$V_{ij} = a\Delta\delta_{ij} + 2\mu D_{ij} \quad (3.2)$$

Where, μ and a are two material properties (which are constants). μ is the first coefficient of viscosity or simply viscosity and (a+2μ/3) is the second coefficient of viscosity or bulk viscosity. D_{ij} is the rate of change of deformation tensor and it can be expressed as

$$D_{ij} = \frac{1}{2}\left(\frac{\partial v_i}{\partial y_j} + \frac{\partial v_j}{\partial x_i}\right) and\ \Delta = D_{11} + D_{22} + D_{33} \quad (3.3)$$

Thus, the total stress tensor can be written as

$$T_{ij} = -p\delta_{ij} + a\Delta\delta_{ij} + 2\mu D_{ij} \quad (3.4)$$

Bulk viscosity (a+2μ/3) becomes zero for fluid which is compressible. Thus, eq. (3.4) can be written as

$$T_{ij} = -p\delta_{ij} - \frac{2\mu}{3}\Delta\delta_{ij} + 2\mu D_{ij} \quad (3.5)$$

If the viscosity of fluid is neglected, eq. (3.5) becomes

$$T_{ij} = -p\delta_{ij} \quad (3.6)$$

Generalized Navier-Stokes's equation of motion is given by

$$\rho\left(\frac{\partial v_i}{\partial t} + v_j\frac{\partial v_i}{\partial x_j}\right) = \frac{\partial T_{ij}}{\partial x_j} + \rho B_i \quad (3.7)$$

Where, body force is denoted by B_i and ρ is the mass density of fluid. Substituting eq. (3.6) in eq. (3.7) the following equations are coming as

$$\rho\left(\frac{\partial v_i}{\partial t}+v_j\frac{\partial v_i}{\partial x_j}\right)=\rho B_i+\frac{\partial \tau_{ij}}{\partial x_j} \tag{3.8}$$

Where the velocity components along x and y axes respectively are u and v and f_x and f_y are body forces along x and y direction respectively and neglecting the convective terms, the equation of motion can be expressed as

$$\frac{1}{\rho}\frac{\partial p}{\partial x}+\frac{\partial u}{\partial t}=f_x \tag{3.9}$$

$$\frac{1}{\rho}\frac{\partial p}{\partial y}+\frac{\partial v}{\partial t}=f_y \tag{3.10}$$

If the body forces are neglected, eqs. (3.9) and (3.10) becomes

$$\frac{1}{\rho}\frac{\partial p}{\partial x}+\frac{\partial u}{\partial t}=0 \tag{3.11}$$

$$\frac{1}{\rho}\frac{\partial p}{\partial y}+\frac{\partial v}{\partial t}=0 \tag{3.12}$$

The continuity equation of fluid in two dimensions is expressed as:

$$\frac{\partial p}{\partial t}+\rho c^2\left(\frac{\partial u}{\partial x}+\frac{\partial v}{\partial y}\right)=0 \tag{3.13}$$

Where, the acoustic wave speed in fluid is denoted as c. Now, differentiating eqs. (3.11) and (3.12) with respect to x and y respectively, the following relations are obtained

$$\frac{1}{\rho}\frac{\partial^2 p}{\partial x^2}+\frac{\partial}{\partial x}\left(\frac{\partial u}{\partial t}\right)=0 \tag{3.14}$$

$$\frac{1}{\rho}\frac{\partial^2 p}{\partial y^2}+\frac{\partial}{\partial y}\left(\frac{\partial v}{\partial t}\right)=0 \tag{3.15}$$

Adding eq. (3.14) and eq. (3.15) we get the following expression

$$\frac{1}{\rho}\frac{\partial^2 p}{\partial x^2}+\frac{1}{\rho}\frac{\partial^2 p}{\partial y^2}+\frac{\partial}{\partial x}\left(\frac{\partial u}{\partial t}\right)+\frac{\partial}{\partial y}\left(\frac{\partial v}{\partial t}\right)=0 \tag{3.16}$$

Differentiating eq. (3.13) with respect to time, the following expression can be obtained

$$\frac{\partial^2 p}{\partial t^2}+\rho c^2\left\{\frac{\partial}{\partial x}\left(\frac{\partial u}{\partial t}\right)+\frac{\partial}{\partial y}\left(\frac{\partial v}{\partial t}\right)\right\}=0 \tag{3.17}$$

Thus, from eq. (3.16) and eq. (3.17), we can find the following expression:

$$\frac{1}{\rho}\frac{\partial^2 p}{\partial x^2} + \frac{1}{\rho}\frac{\partial^2 p}{\partial y^2} - \frac{1}{\rho c^2}\frac{\partial^2 p}{\partial t^2} = 0 \qquad (3.18)$$

Simplifying the eq. (3.18), the equation for compressible fluid may be obtained

$$\nabla^2 p(x,y,t) = \frac{1}{c^2}\ddot{p}(x,y,t) \qquad (3.19)$$

Neglecting the compressibility of fluid, the eq. (3.19) will become

$$\nabla^2 p(x,y,t) = 0 \qquad (3.20)$$

The distribution of pressure in the fluid domain can be obtained by solving eq. (3.19) with the following boundary conditions. Geometry of a typical tank-water system is shown in Fig. 4.1.

i) At surface I

Considering the effect of surface wave of the fluid, the boundary condition of the free surface is taken as

$$\frac{1}{g}\ddot{p}\frac{\partial p}{\partial y} = 0 \qquad (3.21)$$

ii) At surface II and surface IV

At water-tank wall interface, the pressure should satisfy

$$\frac{\partial p}{\partial n}(0,y,t) = \rho_f a e^{iwt} \qquad (3.22)$$

Where ae^{iwt} is representing the horizontal component of the ground acceleration in which, ω can be interpreted as the circular frequency of vibration and $i = \sqrt{-1}, n$ is the outwardly directed normal to the element surface along the interface. *The* mass density of the fluid is denoted by ρ_f

iii) At surface III

This surface is considered to be rigid and thus pressure should satisfy the following condition.

$$\frac{\partial p}{\partial n}(x,0,t) = 0 \qquad (3.23)$$

3.2 Finite Element Formulation

By using Galerkin approach and assuming pressure to be the nodal unknown variable, the discretized form of eq. (3.19) may be written as

$$\int_{\Omega} N_{rj}\left[\nabla^2 \sum N_{ri} p_i - \frac{1}{c^2} N_{ri}\ddot{p}\right] d\,\Omega = 0 \qquad \textbf{(3.24)}$$

Where, N_{rj} is the interpolation function for the reservoir and Ω is the region under consideration. Using Green's theorem eq. (3.24) may be transformed to

$$-\int_{\Omega}\left[\frac{\partial N_{rj}}{\partial x}\sum\frac{\partial N_{ri}}{\partial x}p_i + \frac{\partial N_{rj}}{\partial y}\sum\frac{\partial N_{ri}}{\partial y}p_i\right]d\Omega - \frac{1}{c^2}\int_{\Omega} N_{rj}\sum N_{ri}d\Omega\ddot{p}_i + \int_{\Gamma} N_{rj}\sum\frac{\partial N_{rj}}{\partial n}d\Omega p_i = 0 \qquad \textbf{(3.25)}$$

in which i varies from 1 to total number of nodes and the boundaries of the fluid domain is represented by Γ. The last term of the above equation may be written as

$$\{B\} = \int_{\Gamma} N_{rj}\sum\frac{\partial N_{rj}}{\partial n}d\Omega p_i \qquad \textbf{(3.26)}$$

The whole system of equation (3.25) may be written in a matrix form as

$$[\vec{E}]\{\ddot{P}\} + [G]\{P\} = \{F\} \qquad \textbf{(3.27)}$$

Where,

$$[\vec{E}] = \frac{1}{c^2}\sum\int_{\Omega}[N_r]^T[N_r]d\Omega \qquad \textbf{(3.28)}$$

$$[\vec{G}] = \sum\int_{\Omega}\left[\frac{\partial}{\partial x}[N_r]^T\frac{\partial}{\partial x}[N_r] + \frac{\partial}{\partial y}[N_r]^T\frac{\partial}{\partial y}[N_r]\right]d\Omega \qquad \textbf{(3.29)}$$

$$\{F\} = \sum\int_{\Gamma}[N_r]^T\frac{\partial p}{\partial n}d\Gamma = \{F_I\} + \{F_{II}\} + \{F_{III}\} + \{F_{IV}\} \qquad \textbf{(3.30)}$$

Here different surface conditions are denoted by the subscripts I, II, III, IV. The eq. 3.21 can be written in finite element form for surface wave as,

$$\{F_I\} = -\frac{1}{g}[R_f]\{\ddot{p}\} \qquad \textbf{(3.31)}$$

Where,

$$[R_f] = \sum\int_{\Gamma_f}[N_r]^T[N_r]\,d\Gamma \qquad \textbf{(3.32)}$$

At the Surface II and Surface IV if {a} is the vector of nodal accelerations of generalized coordinates, $\{F_{II}\}$ and $\{F_{IV}\}$ may be expressed as,

$\{F_{II}\}$ and $\{F_{IV}\}$= -ρ$[R_{II}]${a} and -ρ$[R_{IV}]${a} respectively (3.33)

$[R_{II}]$ and $[R_{IV}] = \sum \int_{\Gamma_{I\ and\ IV}} [N_r]^T [N_r]\, d\Gamma$ (3.34)

At Surface III,

$\{F_{III}\} = 0$ (3.35)

After substitution all terms the eq. (3.27) becomes

$[E]\{\ddot{P}\} + [G]\{P\} = \{F_r\}$ (3.36)

Where,

$[E] = [\vec{E}] + \frac{1}{g}[R_I]$ (3.37)

$\{F_{IV}\}$= - ρ$[R_{II}]${a} - ρ$[R_{IV}]${a} (3.38)

For any given acceleration at the fluid-structure interface, the hydrodynamic pressure within the fluid is obtained by solving the eq. (3.26).

3.3 Time History Analysis of dynamic equilibrium equation

Dynamic equilibrium equation of fluid can be expressed as

$[E]\{\ddot{P}\} + [G]\{P\} = \{F_r\}$ (3.36)

These values remain constant throughout the time history analysis of a linear dynamic system. The force vector is expressed as $\{F_r\}$. To obtain the transient response at time t_N, the time axis can be discredited into N equal time intervals ($t_N = \sum_{j=1}^{N} j\Delta t$). The choice of method for time-history analysis is strongly dependent on the problem. Various direct time integration methods exist for time history analysis that are expedient for structural dynamics and wave propagation problem. Amongst these, the most popular is the Newmark family of methods and it is given by

$\{p\ \}_{j+1} = \{p\ \}_j + \Delta t\{\dot{p}\}_j + \frac{\Delta t^2}{2}[(1-2\vartheta)\{p\}_j + 2\vartheta\{\ddot{p}\}_{j+1}]$ (3.39)

$\{\dot{p}\}_{j+1} = \{\dot{p}\}_j + \Delta t[(1-\gamma)\{\ddot{p}\}_j + \gamma\{\ddot{p}\}_{j+1}]$ (3.40)

Here, ϑ and γ are taken to control stability and accuracy. It is evident from the literature that the integration scheme is unconditionally stable if $2\vartheta \geq \gamma \geq 0.5$.

3.3.1 Stability Analysis of Newmark Method

The numerical integration of time in the finite element system equilibrium equations is performed to approximate the actual dynamic response of the system under consideration. Stability of an integration scheme implies that the initial conditions for the equations with a large value of Δt /T must not be amplified artificially. In a stable scheme, the abrupt increase of any errors in displacements, velocities and accelerations at time t is not present, due to rounding off during computation. Stability is acquired if the time step chosen is small enough to integrate the response accurately in the highest frequency component. It is important to optimize the size of the time step, so as to obtain accuracy but at the same time to avoid an increase in computational cost.

3.3.2 Accuracy Analysis of Newmark Method

The choice of the integration operator depends on the cost of solution in a practical analysis and that is determined by the number of time step required in the integration. For a conditionally stable algorithm such as central difference, the time steps for a given time range considered is determined by the critical time step Δt_{cr} and there is not many choices that are available. The errors in the integration can be measured in terms of period elongation and amplitude decay. The various integration methods exhibit quite different characteristics, when the time step to period ratio is large. The Wilson-θ method with $\theta = 1.4$ introduces less amplitude decay and period elongation than the Houbolt method for a given Δt /T, and the Newmark average acceleration method introduces only period elongation and no amplitude decay. If the Newmark constant average acceleration is employed, the high frequency response is retained in the solution. The most desirable stability is obtained for the method corresponding to $\gamma = 0.5$ and $\vartheta = 0.25$. Therefore, in the present work, the dynamic equilibrium equations are solved using the values of γ and ϑ as 0.5 and 0.25 respectively.

3.4 Computation of Velocity and Displacement of Fluid

The accelerations of the fluid particles can be calculated after we compute the hydrodynamic pressure in the water tank. The velocity of the fluid particle can be calculated from the known values of acceleration at any instant of time using Gill's time integration scheme (Gill 1951) which is a step-by-step integration procedure that is based on Runge-Kutta method (Ralston and Wilf 1965). This procedure has several advantages over the other available methods as it (i) needs less storage registers, (ii) controls the growth of rounding errors, (iii) is usually stable and (iv) is computationally economical. At any instant of time t, velocity can be expressed as

$$V_t = V_{t-\Delta t} + \Delta t \dot{V}_t \qquad (3.41)$$

Velocity vectors in the fluid domain may be plotted based on velocities computed at the Gauss points of each individual element and then extrapolating to their nodal points. Similarly, the displacement of fluid particles in the fluid domain, U at every time instant can also be computed as

$$U_t = U_{t-\Delta t} + \Delta t V_t \qquad (3.42)$$

CHAPTER 4

RESULTS AND DISCUSSIONS

4.1 Validation of the Proposed Algorithm.

In this section, a bench marked problem is solved and results are compared with the results obtained by Virella et al. (2008) to determine the accuracy of present algorithm. The geometric and material properties of the tank are as follows: height of water in the tank (H) = 6.10 m, length of tank (L) = 30.5 m, so that ratio of height to length (H/L) = 0.2, density of water = 983 kg/m^3, pressure wave velocity = 1451 m/s. Here, the fluid is discretized by 4 ×8 (i.e., N_h= 4 and N_v = 8).The first three natural time periods of the tank fluid are listed and compared with those values obtained by Virella et al. (2008) in Table 4.1. The tabulated results show the accuracy of the present method.

Table 4.1 First three natural time period of the tank fluid

Mode number	Natural Time period in sec	
	Present Study	Virella et al. (2008)
1	8.396	8.38
2	3. 729	3.70
3	2.823	2.78

4.2 Selection of Time Step

The results from Newmark's integration technique are quite sensitive to the time step and to determine a suitable time step, tank with following properties are considered. Water depth (H) = 2.0 m, length of tank (L) =1.0 m, acoustic speed (C) = 1440 m/sec, mass density of water (ρ) = 1000 kg/m^3. The study is carried out against sinusoidal excitation of frequencies 30.0 rad/sec, 7.0 rad/sec and 1.5 rad/sec with amplitude of 1.0g. Here, the fluid domain is discretized by 4 × 8 (i.e., N_h = 5 and N_v = 10) (Fig. 4.1). Tank walls and the base are assumed to be rigid. The maximum hydrodynamic pressure coefficient (C_p = P /ρ*Amp*H) for different number of time step (N_t) for different exiting frequencies are summarized in Table

4.2. It is observed from the tabular results that the developed hydrodynamic pressure for different exciting frequencies is converged for values of N_t= 32. Thus, the time step (Δt) for the analysis of water tank is adopted as T/32 (T=time period) for all the case unless it is mentioned.

Table 4.2 Convergence of hydrodynamic pressure coefficients (C_p) for different time steps

N_t	Exciting frequency		
	30.0 rad/sec	7.0rad/sec	1.5rad/sec
8	0.6125	8.9612	2.3618
16	0.6264	9.8750	2.6730
24	0.6396	9.9436	2.5619
32	0.6479	9.9147	2.6324
64	0.6479	9.9147	2.6324
128	0.6479	9.9147	2.6324

4.3 Selection of Suitable Mesh Size

To obtain a suitable mesh size, tank with following properties are considered. Water depth (H) = 2.0 m, length of tank (L) =0.8 m acoustic speed (C) = 1440 m/sec, mass density of water (ρ) = 1000 kg/m^3. The study is carried out for an exciting frequency of *1.50 rad/sec* with amplitude of 1.0 g. The maximum pressure coefficient ($C_p = p/\rho*Amp*H$) for different mesh size are summarized in Table 4.3. From Table 4.3 it is observed that the maximum hydrodynamic pressure is converged when the horizontal division (N_h) is equal or higher than 4 and the ratio of vertical division to horizontal division (N_v/N_h) is equal to 1.0. However, for further numerical study, N_h is consider as 4 and the higher value (Fig 4.2). The values N_h and N_v are mention in respective examples.

Table 4.3 Convergence of hydrodynamic pressure coefficients (C_p) for different mesh size

Mesh Size ($N_h \times N_v$)	N_v/N_h	Pressure coefficient (P/(apd))

(1 ×1)	1	1.6987
(1 ×2)	2	1.6619
(2×1)	0.5	1.8775
(2 ×2)	1	1.9790
(3 ×1)	0.33	1.9986
(3 ×2)	0.67	2.0548
(3 ×3)	1	2.0978
(4 ×2)	0.5	2.1087
(4 ×3)	0.75	2.2431
(4 ×4)	1	2.6324
(4 ×6)	1.5	2.6324
(6 ×6)	1	2.6324

4.4 Analysis of liquid containers against different earthquake excitations

The impulsive responses of tanks with different sizes are determined against two different earthquake excitations. The external excitations considered in the study are Koyna earthquake (Fig.1) and Taft earthquake (Fig. 2). In this section, the impulsive responses of tank with different sizes due to two different earthquake excitations are studied. The material properties for water with in the tank are follows: acoustic speed in water (α) = 1440 m/sec, mass density of water (ρ_f) = 1000 kg/m^3, Length of tanks (L) =20m. However, different heights (H), such as 5m (H/L=0.25), 10m (H/L=0.5), 20m (H/L=1.0), 30m (H/L=1.5) and 40m (H/L=2.0) are considered. In the present study, tank walls are considered to be rigid. The water in the tanks is discretized by 10 × 10 (i.e., N_h = 10 and N_v = 10) as obtained in the section 4.3.

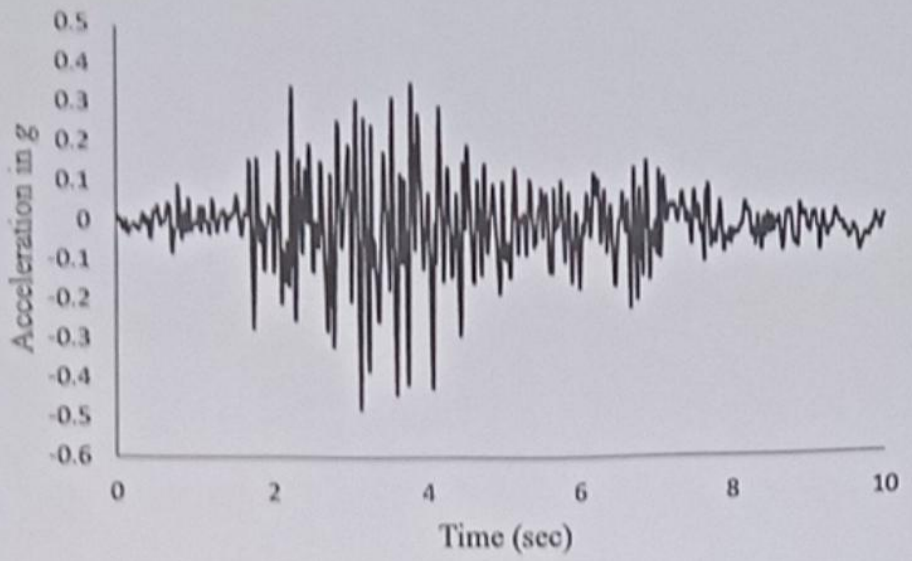

Fig 4.1 Acceleration of Koyna earthquake

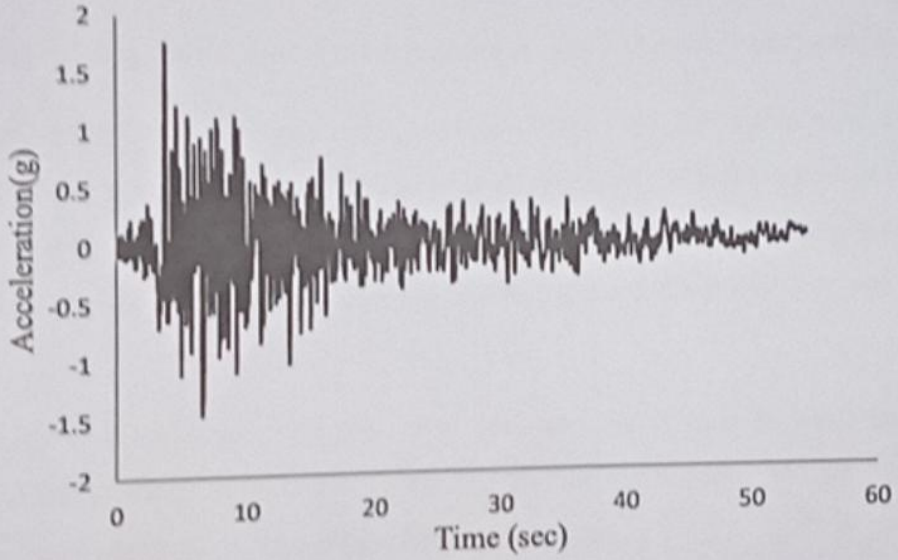

Fig 4.2 Acceleration of Taft earthquake

Impulsive hydrodynamic pressure at the free surface of liquid for Koyna earthquake is plotted in Fig. 4.3 From Fig.4.3, it is clear that impulsive hydrodynamic pressure for all heights of the tank follows almost similar pattern. However, the impulsive hydrodynamic pressure increases with the increase of tank height and maximum hydrodynamic pressure is obtained when tank height is 40m.

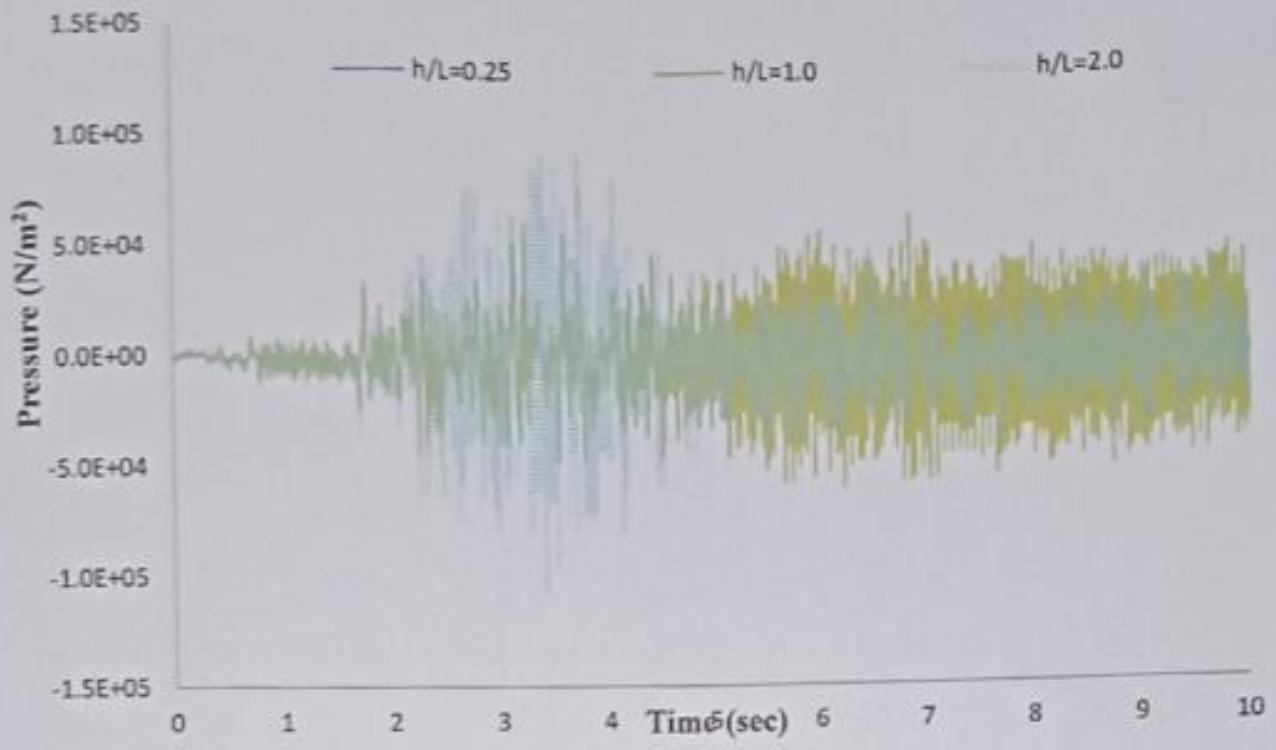

Fig 4.3 Impulsive hydrodynamic pressure due to Koyna Earthquake

Impulsive hydrodynamic pressure at the free surface of liquid for Taft earthquake is plotted in Fig. 4.4. From Fig.4.4, it is clear that impulsive hydrodynamic pressure for all heights of the tank follows almost similar pattern. However, the impulsive hydrodynamic pressure increases with the increase of tank height and maximum hydrodynamic pressure is obtained when tank height is 40m.

From the figures it is clear that the nature of pressure distribution is same for both the earthquakes but the intensity of pressure is more for the Taft earthquake. We will discuss how this affects the other parameters for the two earthquake cases.

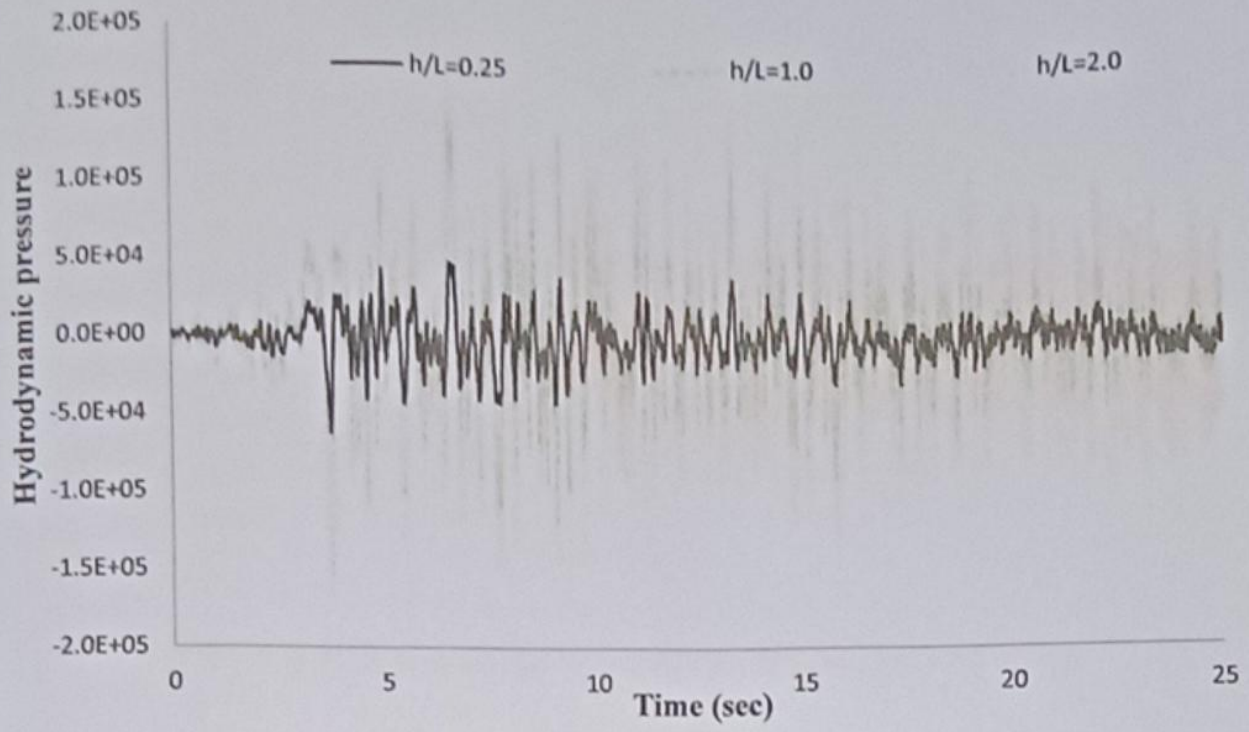

Fig. 4.4 Impulsive hydrodynamic pressure due to Taft Earthquake

Impulsive hydrodynamic pressure along the tank walls due to Koyna and Taft earthquake are also plotted in Fig.4.5 to Fig. 4.9. These figures depict that the maximum impulsive hydrodynamic pressure occurs at the bottom of the tank and it gradually decreases towards the free surface of the tank and this decrease in impulsive hydrodynamic pressure is more rapid for comparatively higher for tank with more height. It is also noticeable that the impulsive hydrodynamic pressure at the free surface decreases with the increase of tank height. On the other hand, the impulsive hydrodynamic pressure at the base of the tank has a higher magnitude for comparatively more height of tanks. Impulsive hydrodynamic pressure at the free surface of tank is almost zero for different tank heights. However, tanks with different heights have maximum impulsive hydrodynamic pressure at the base for both the earthquakes. It is noticeable that the maximum pressure is more for the Taft earthquake for any height of the tank.

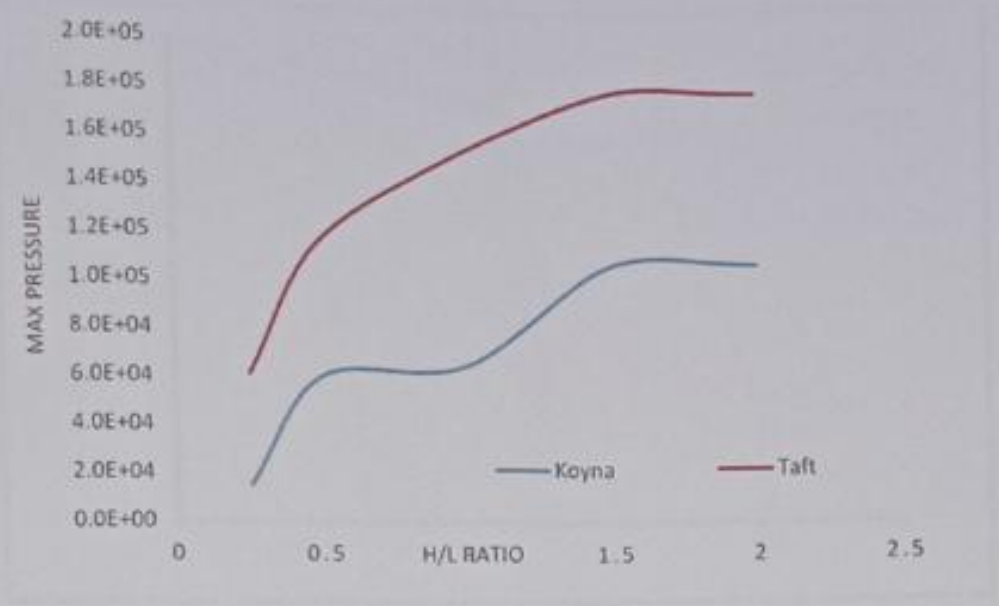

Fig. 4.5 Impulsive hydrodynamic pressure for different h/L ratio of tank

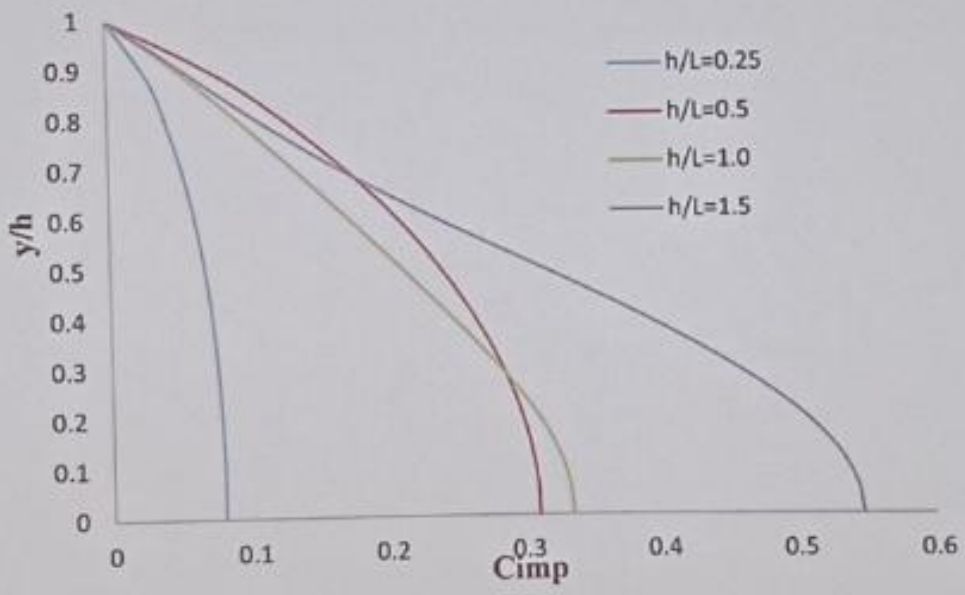

Fig. 4.6 Impulsive hydrodynamic pressure on the left wall of the tank due to Koyna earthquake

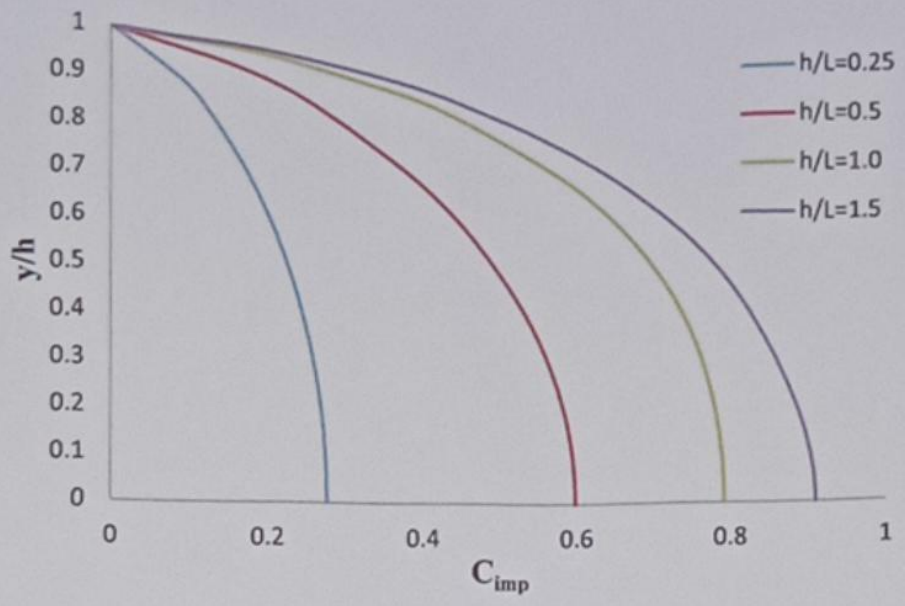

Fig. 4.7 Impulsive hydrodynamic pressure on the left wall of the tank due to Taft earthquake

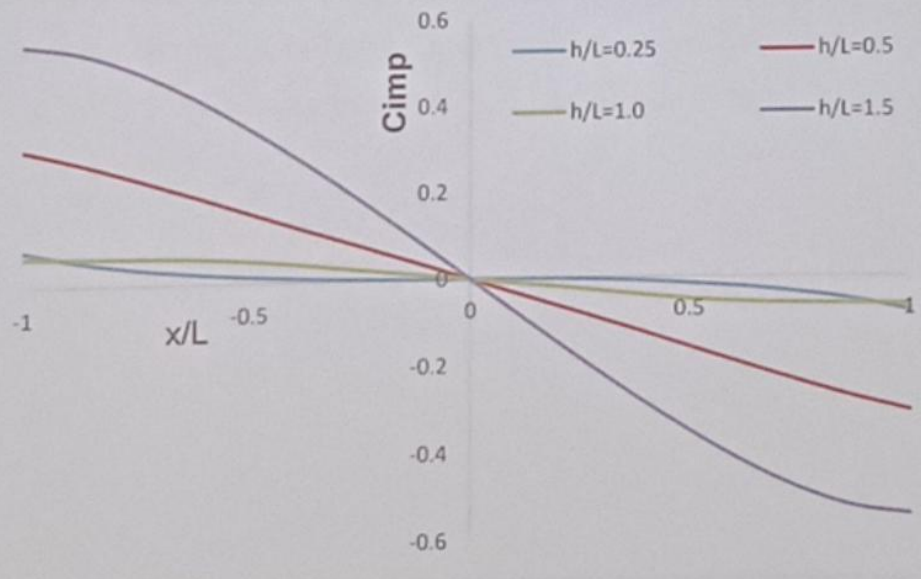

Fig. 4.8 Impulsive hydrodynamic pressure on bottom of the tank due to Koyna earthquake

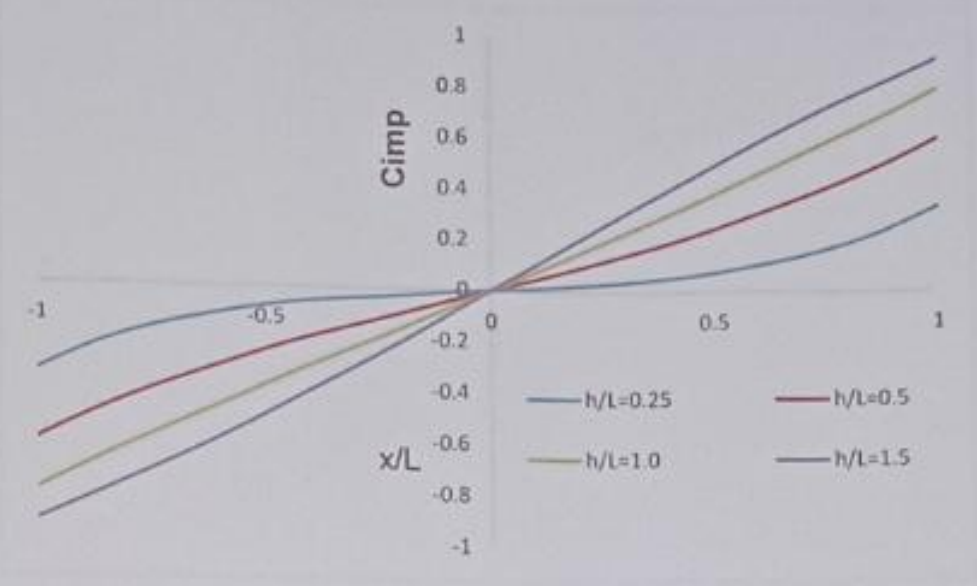

Fig. 4.9 Impulsive hydrodynamic pressure on bottom of the tank due to Taft earthquake

The impulsive hydrodynamic pressure at a height of 2.5m and 5m from the base of tank has been plotted for Koyna and Taft Earthquake. As the height of the tank is increasing, the impulsive hydrodynamic pressure is also increasing at a constant depth of tank. One point is to be noted here that the impulsive hydrodynamic pressure is less for a height of 5m than the at the height of 2.5m from the base of tank for any fixed height of tank.

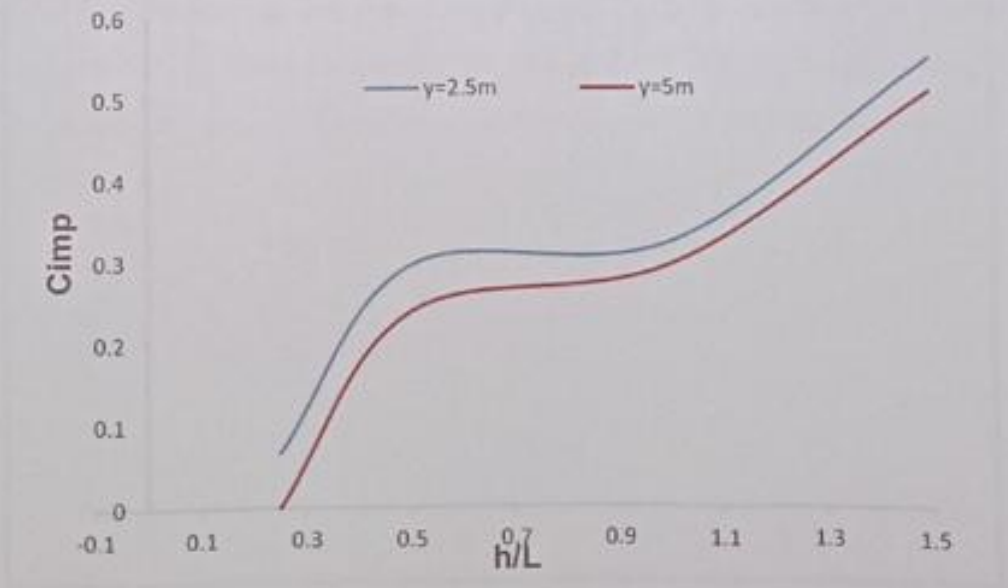

Fig. 4.10 Impulsive hydrodynamic pressure at a depth 2.5m and 5.0m due Koyna earthquake

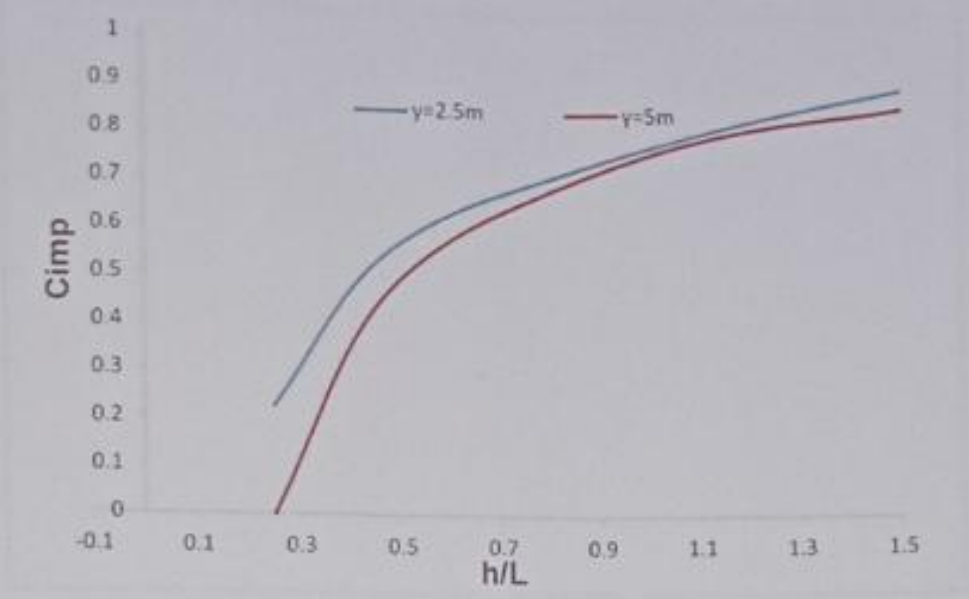

Fig. 4.11 Impulsive hydrodynamic pressure at a depth 2.5m and 5.0m due Traft earthquake

Velocity profile for different height of tanks against Koyna and Taft earthquake excitement are plotted in Fig 4.12 and Fig 4.13. Due to external excitation, the entire liquid within the container is disturbed (Fig 4.12)). However, the disturbance is concentrated near the free surface for comparatively higher tank height and the bottom surface stayed comparatively calm. The disturbance near the free surface is more for comparatively higher h/L ratio. For h/L ratio equal to 1.0 and more, the liquid after certain depth remains almost undisturbed. It is to be noted the velocity profile of tank remained unchanged for both the earthquake excitations.

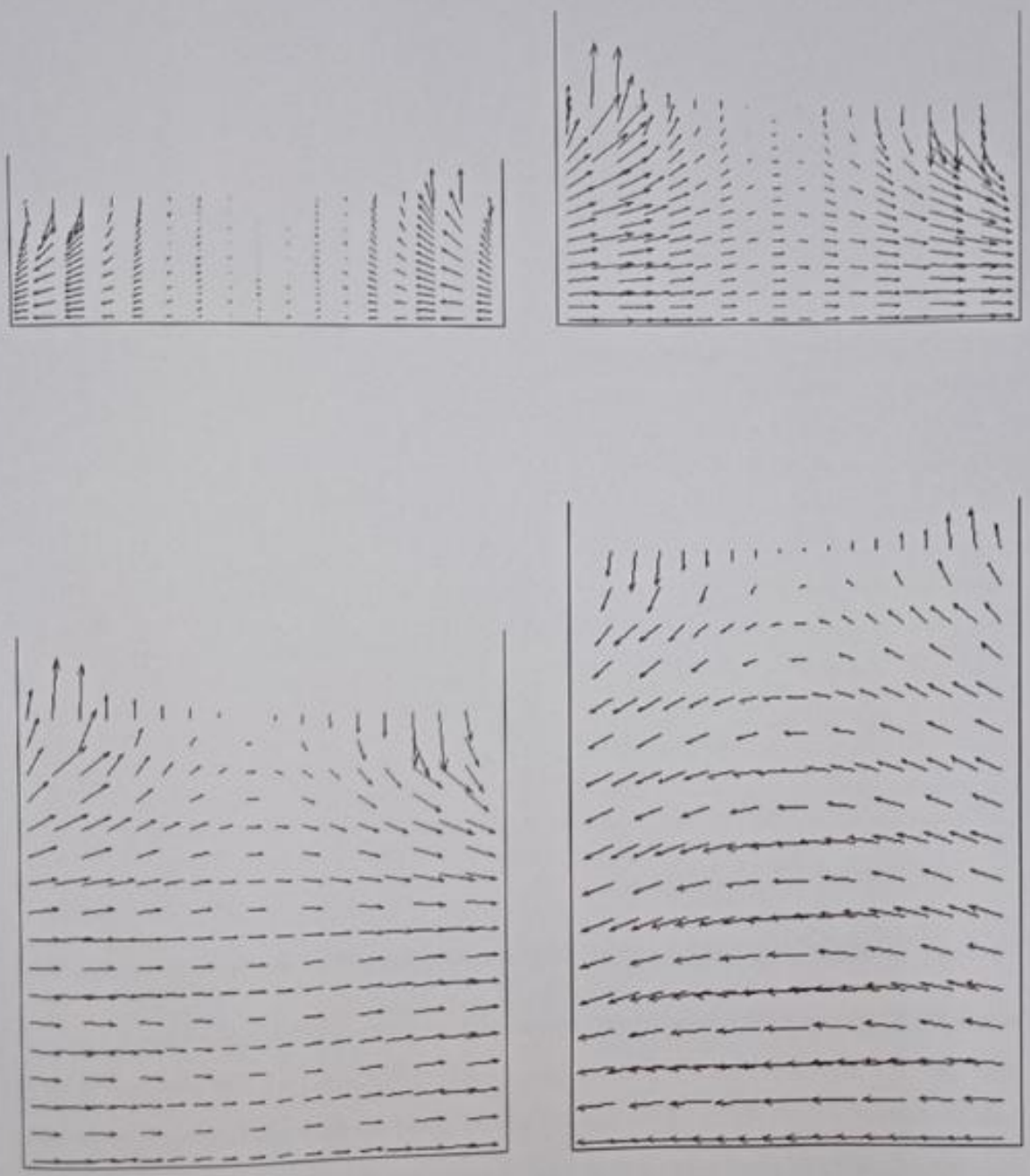

Fig. 4.12 Velocity profile of tanks due Koyna earthquake

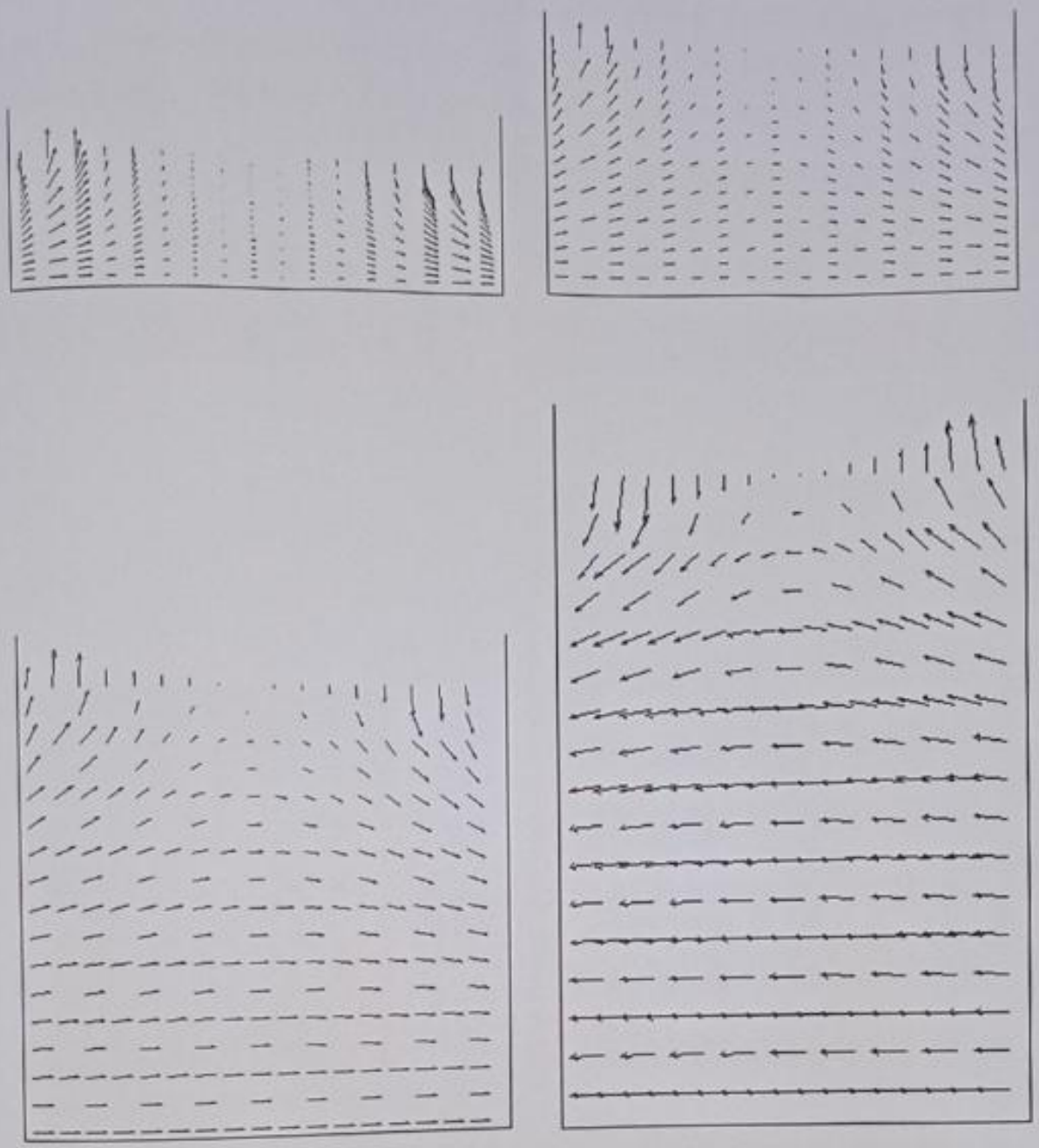

Fig. 4.13 Velocity profile of tanks due to Taft earthquake

Pressure contours for different tank heights are presented in Fig 4.15 and Fig 4.16. From Figure it is clear that the impulsive pressure is more near the tank wall and it is almost zero near the midpoint of the tank for both the earthquakes. We can also see from this figure that the impulsive pressure is distributed almost through the entire tank. The distribution of impulsive pressure changes when h/L changes (Fig4.14). The impulsive hydrodynamic pressure near the tank wall increases with the increase of tank height and the distribution pattern of this pressure near tank wall is smooth for comparatively lower tank height. The

depth of undisturbed zone which is presented in blue colour (Fig. 4.14(i)-(iv)). It increases with the increase of h/L ratio. The patterns are similar for both the earthquakes. But the pressure intensity is more for Taft earthquake than Koyna earthquake.

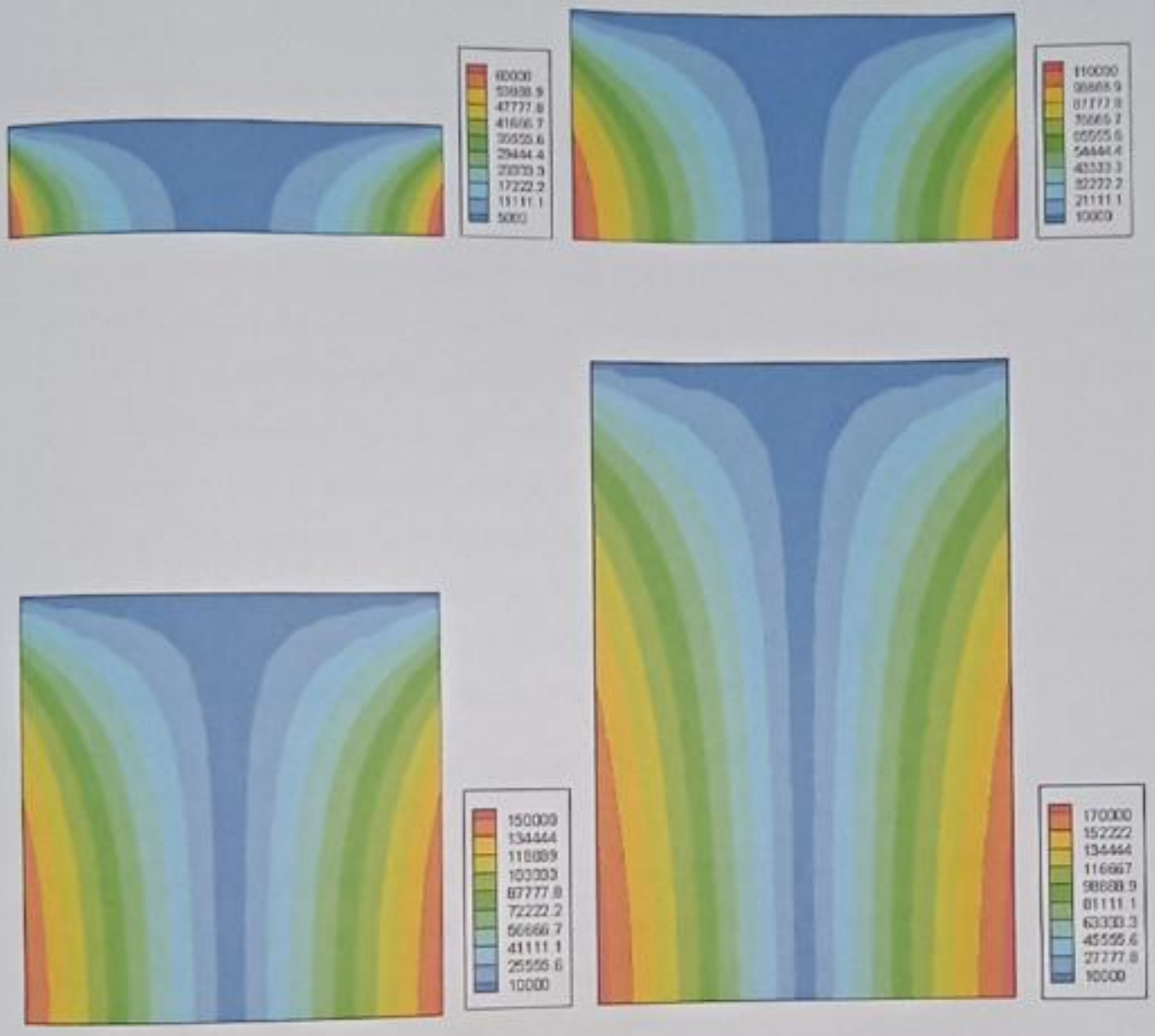

Fig. 4.14 Pressure contour due to Taft earthquake

CHAPTER 5
CONCLUSIONS

The impulsive hydrodynamic pressure of rectangular water tank against different exciting frequencies have been studied here. The liquid within the tank is considered to be incompressible. A pressure based finite element method is used to simulate the liquid in the tank and walls of tank are considered to be rigid.

The impulsive hydrodynamic pressure on the walls and displacement at the free surface of liquid are considered to the main aspect during design of such tanks. In the present study, the impulsive hydrodynamic pressure on vertical walls of different sizes at different heights against different exciting frequencies is determined. The impulsive hydrodynamic pressure within tank depends on exciting frequencies as well as the height of rectangular water tank. The impulsive hydrodynamic pressure at base and mid height of vertical wall increases with the increase of height of liquid within tank. The pressure at the base also increases with the increase of tank height. Hydrodynamic pressure at a constant depth of tank also increases with the increase of height of tank.

The disturbance at free surface depends on height of tank. It also depends on exciting frequency. The disturbance increases with the increase of exciting frequency and has maximum value at the free surface of the tank. However, the disturbance is getting reduced as depth of our observation increases in the tank. The disturbance at the free surface is more as the height of the tank increases. The impulsive hydrodynamic pressure is maximum near the walls and zero at midpoint of the tank for a constant depth.

5.1 Future Scope of Work

The present work is an investigation of impulsive responses of rectangular water tank against different earthquake excitations. There are certain other aspects that may be considered for further research:

- The present study is limited to the finite element analysis of fluid domain only. The study may be further extended considering flexibility of tank wall and fluid-structure interaction.
- The present problem may be extended to 3-dimensional form with and without fluid-structure interaction.
- The analysis may also be performed for cylindrical and other types of tank. Different types of baffle such ring type and horizontal may be used within the tank.
- Non-linear wave theory may be used to simulate the water or other fluid motion within the tank.

References:

P. Deepak Kumar, Aishwarya Alok, P.R. Maiti, *Comparative Study of Dynamic Analysis of Rectangular Liquid Filled Containers Using Codal Provisions,* Procedia Engineering 144 (2016) 1180 – 1186.

J.H. Jung, H.S. Yoon, C.Y. Lee, S.C. Shin, *Effect of the vertical baffle height on the liquid sloshing in a three-dimensional rectangular tank,* Ocean Engineering 44 (2012) 79-89.

Lenka Uhlirova, Norbert Jendzelovsky, *Dynamic analysis of rectangular tank using response spectra,* Vibroengineering PROCEDIA, Vol. 23, 2019, p. 99-104.

XUE Mi-an, LIN Peng-zhi, ZHENG Jin-hai, MA Yu-xiang, YUAN Xiao-li, Viet-Thanh NGUYEN, *Effects of Perforated Baffle on Reducing Sloshing in Rectangular Tank: Experimental and Numerical Study,* China Ocean Eng., Vol. 27, No. 5, pp. 615 – 628.

Akyildiz, H. (2012), *A numerical study of the effects of the vertical baffle on liquid sloshing in two-dimensional rectangular tank,* Journal of Sound and Vibration, 331(1), 41–52.

Y.G. Chen, K. Djidjeli, W.G. Price, *Numerical simulation of liquid sloshing phenomena in partially filled containers,* Computers & Fluids 38 (2009) 830–842.

Hakan Akyildiz; Erdem Ünal (2005). *Experimental investigation of pressure distribution on a rectangular tank due to the liquid sloshing,* Ocean Engineering 32 (2005) 1503–1516.

P. Pal; S.K. Bhattacharyya (2010). *Sloshing in partially filled liquid containers—Numerical and experimental study for 2-D problems,* Journal of Sound and Vibration 329 (2010) 4466–4485.

K. C. Biswal; S. K. Bhattacharyya; P. K. Sinha (2006). *Non-linear sloshing in partially liquid filled containers with baffles,* Int. J. Numer. Meth. Engng 2006; 68:317–337.

Brar, Gurinder Singh; Singh, Simranjit, *An Experimental and CFD Analysis of Sloshing in a Tanker,* Procedia Technology, 14(2014), 490–496.

Hakan Akyildız; N. Erdem Ünal, *Sloshing in a three-dimensional rectangular tank: Numerical simulation and experimental validation,* Ocean Engineering 33 (2006) 2135–2149.

Y Kim (2001). *Numerical simulation of sloshing flows with impact load,* Applied Ocean Research 23 (2001) 53-62.

Nicolici, S.; Bilegan, R.M., *Fluid structure interaction modeling of liquid sloshing phenomena in flexible tanks*. Nuclear Engineering and Design, 258(2013), 51–56.

Dongming Liu; Pengzhi Lin, *Three-dimensional liquid sloshing in a tank with baffles,* Ocean Engineering 36 (2009) 202–212.

Hou, L., Li, F., & Wu, C. (2012). *A numerical study of liquid sloshing in a two-dimensional tank under external excitations*. Journal of Marine Science and Application, 11(3), 305–310.

Kamila Kotrasová, Eva Kormaníková, Slávka Harabinová, Mohamed Loukili, *Pressure analysis of rectangular fluid filling,* 2020 24th International Conference on Circuits, Systems, Communications and Computers (CSCC).

A. Doğangün; A. Durmuş; Y. Ayvaz (1996). *Static and dynamic analysis of rectangular tanks by using the lagrangian fluid finite element.* Computers & Structures, 59(3), 547–552.

Y.G. Chen; K. Djidjeli; W.G. Price (2009). *Numerical simulation of liquid sloshing phenomena in partially filled containers, Computers & Fluids 38 (2009) 830–842.*

Ping-jian MING; Wen-yang DUAN (2010). *Numerical simulation of sloshing in rectangular tank with VOF based on unstructured grids,* Journal of Hydrodynamics 22(6) 856-864.

S. Mitra; K.P. Sinhamahapatra (2008). *2D simulation of fluid-structure interaction using finite element method,* Finite Elements in Analysis and Design 45 (2008) 52 – 59.

J. C. Virella et al. "Effect of pre-stress states on the impulsive modes of vibration of cylindrical tank-liquid systems under horizontal motions", Vibration and Control 11(9) (2005) 1195- 1220

Ralston A,Wilf HS. Mathematical Models for Digital Computers, Wiley1965; New York.

Gill S. A process for the step-by-step integration of differential equations in an automatic digital computing machine, Proceedings of the Cambridge Philosophical Society1951;47: 96-108.